

studied theoretically [R. J. Joenk, Phys. Rev. **128**, 1634 (1962)] and experimentally [J. H. Schelleng and S. A. Friedberg, J. Appl. Phys. **34**, 1987 (1963)] in terms of applied fields in the neighborhood of the spin-flop transition. To our knowledge the present cooling effect in the neighborhood of the spin-flop to paramagnetic transition has not been discussed in the literature. See, however, the work of T. A. Reichert, R. A. Butera, and E. J. Schiller, Phys. Rev. B **1**, 4446 (1970).

¹²M. F. Panczyk and E. D. Adams, Phys. Rev. **187**, 321 (1969).

¹³W. R. Abel, A. C. Anderson, W. C. Black, and J. C.

Wheatley, Phys. Rev. **147**, 111 (1966).

¹⁴G. A. Baker, Jr., H. E. Gilbert, J. Eve, and G. S. Rushbrooke, Phys. Rev. **164**, 800 (1967).

¹⁵R. A. Scribner, M. F. Panczyk, and E. D. Adams, Phys. Rev. Lett. **21**, 427 (1968).

¹⁶Molecular-field theory is inadequate for the calculation of entropy in the spin-flop region where the excitations are primarily long-wavelength spin waves. In the bcc structure there is a large peak in the density of states at the zone boundary which happens to be at the molecular-field energy. Molecular-field theory then becomes a good approximation over most of the paramagnetic region.

Time-Resolved Light-Scattering Measurements of the Spectrum of Turbulence within a High- β Collisionless Shock Wave

M. Keilhacker and K.-H. Steuer

Max-Planck-Institut für Plasmaphysik—EURATOM Association, Garching bei München, Germany

(Received 9 February 1971)

Strong current-driven turbulence is observed in high- β collisionless shock waves under $T_e \sim T_i$ and $v_d \ll v_e$ conditions. The level and the frequency and wave-number spectra of this turbulence are measured by scattering light from the shock. The turbulence is probably due to an electron-cyclotron drift instability.

Previous experiments^{1,2} on collisionless shock waves have established that the electron heating observed in low-Mach-number shocks ($M < M_{\text{crit}}$, resistive shocks) implies a resistivity in the shock front which is about two orders of magnitude larger than the "classical" value based on binary Coulomb collisions. It is generally presumed that this "anomalous" resistivity is due to scattering of the electrons by suprathermal electrostatic fluctuations arising from some microinstability.

This Letter deals with time-resolved measurements of the level³ and spectrum⁴ of suprathermal fluctuations in a collisionless shock wave. The quasistationary shock, which propagates perpendicular to a magnetic field B_1 with Mach number $M = 2.5$, is produced by radial compression of an initial deuterium plasma by a fast θ pinch.⁵ The initial plasma conditions² ($n_{e1} = 4 \times 10^{14} \text{ cm}^{-3}$, $T_{e1} = 4 \text{ eV}$, $T_{i1} = 18 \text{ eV}$,⁶ $B_1 = 700 \text{ G}$) differ from other shock experiments insofar as the plasma β is high ($\beta_1 \sim 0.7$) and $T_{e1}/T_{i1} < 1$. As a consequence of the latter the electron temperature T_e does not substantially exceed the ion temperature T_i during the shock-heating process ($T_{e2} = 110 \text{ eV}$ from 90° laser scattering, $T_{i2} \sim 70 \text{ eV}$ from Rankine-Hugoniot relations). This makes it unlikely that the microturbulence caus-

ing the observed collisionless electron heating² results from an ion acoustic instability as proposed for other experiments^{7,8} in which $T_e/T_i \gg 1$.

Laser scattering experiments.—In the laser scattering experiments, described in detail elsewhere,^{3,9} the light pulse of a 500-MW ruby laser is timed to hit the shock wave while it traverses the beam. The pulse width (12 nsec) and divergence of the laser beam make it possible to resolve the structure of the shock wave.

The light scattered in the forward direction $\theta = 2.5^\circ - 6^\circ$ is detected by a photomultiplier, either directly or after spectral resolution. The geometry of incident and scattered-light paths is such that the scattering plasma waves have a wave vector \vec{k} —with $|\vec{k}|$ of order $1/D$ ($\alpha \sim 1/|\vec{k}|D \geq 1$), D being the Debye length—collinear with the azimuthal current in the shock front. Simultaneously with the forward-scattering measurements, the density and electron temperature in the shock are determined by 90° scattering ($\alpha \ll 1$) using a multichannel detector arrangement.

Measured level of fluctuations.—Figure 1 shows the measured total level of density fluctuations $n_e S$ as a function of time for a scattering angle $\theta = 2.5^\circ \pm 0.5^\circ$ ($|\vec{k}| = 4 \times 10^3 \text{ cm}^{-1}$). Time is measured from the beginning of the θ -pinch discharge. The experimental points denoted by open cir-

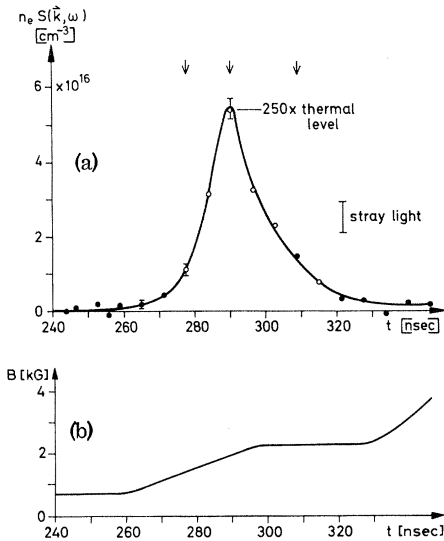


FIG. 1. (a) Intensity of density fluctuations $n_e S(\vec{k}, \omega)$ within a collisionless shock wave (Mach number 2.5, deuterium plasma) reaching 250 times the thermal level. (b) Magnetic field B for time comparison.

cles are mean values of 10 or more measurements, and the error bars are the standard deviation from the mean value. For a time comparison the magnetic field B in the shock wave is also plotted. In the shock front the level of fluctuations is strongly suprathermal, reaching at its maximum about 250 times the thermal value. At the back of the shock the fluctuations decay to the thermal level.

Frequency spectrum of fluctuations. - The frequency spectrum $S_k(\omega)$ of these fluctuations is obtained by spectrally resolving the scattered light using a double Fabry-Perot interferometer (resolution $2 \times 10^{-3} \text{ \AA}$). The total resolution, including the spectral width of the laser line, is $3 \times 10^{-2} \text{ \AA}$. The spectral profiles are scanned shot by shot; the total line intensity, which is measured simultaneously, is used for relative calibration.

Figure 2 shows the frequency spectrum $S_k(\omega)$ of these fluctuations corrected for instrumental width at the three points of time indicated by arrows in Fig. 1. The peaks of the scattered spectra are shifted to the red with respect to the laser line. At all three points of time the absolute value of the shift corresponds to scattering from plasma waves with frequency $\omega \sim 0.5 \omega_{pi}$, where ω_{pi} is the ion plasma frequency. In the shock front the shift increases because of the compression of the plasma and then remains constant.

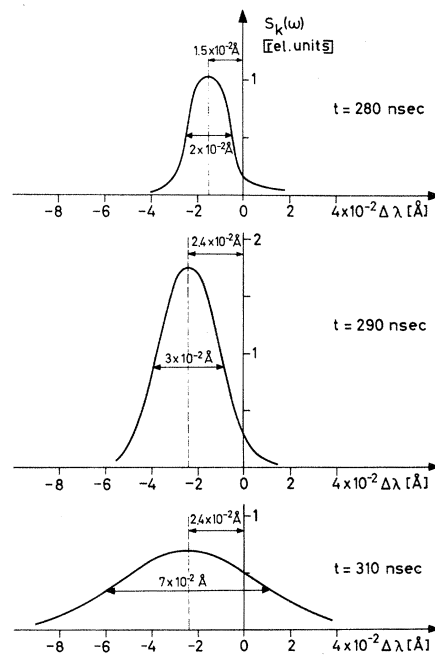


FIG. 2. Frequency spectra $S_k(\omega)$ of enhanced fluctuations for three points of time indicated by arrows in Fig. 1.

The direction of the shift corresponds to scattering from plasma waves traveling in the same direction as the electrons that carry the diamagnetic current in the shock front. This and the further result that the direction of shift reverses if the current is reversed indicate that the electron current drives the instability. The width of the scattered spectra, which increases with time, is comparable to its shift. This means that the lifetime of the unstable modes is comparable with their period. It can be estimated to be about 0.5 nsec.

Wave-number spectrum of fluctuations. - The k spectrum of the enhanced fluctuations was measured by varying the scattering angle θ between 2.5° and 6° . Figure 3 shows the wave-number spectrum $S(k)$ at the time of maximum turbulence together with the form predicted by Kadomtsev.¹⁰ Horizontal bars through the experimental points indicate the finite angle of acceptance of the scattered light, while vertical lines are error bars. The measured spectrum shows a logarithmic cutoff for $k \geq 1/D$ as predicted by Kadomtsev's theory of ion wave turbulence, but the dependence on k seems to be weaker than predicted.

Discussion of results. - The observed reversal of the frequency shift with the reversal of the diamagnetic current in the shock front suggests

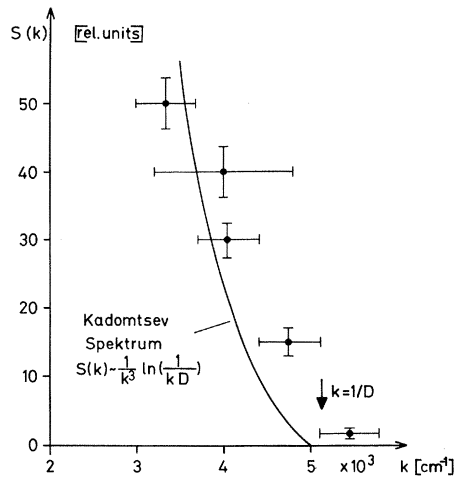


FIG. 3. Wave number spectrum $S(k)$ of enhanced fluctuations at time of maximum turbulence together with the form predicted by Kadomtsev.

that the electron drift is the driving source of the enhanced fluctuations. Therefore the following question arises: Which waves become unstable and grow fast enough under the existing shock conditions to account for the measured level of fluctuations?

The two quantities relevant to this question are the ratio of electron drift velocity to electron thermal velocity v_d/v_e and the ratio of electron to ion temperatures T_e/T_i . The ratio v_d/v_e is about 0.2 at the front of the shock and decreases towards the rear owing to the increasing electron temperature, while T_e/T_i is 0.22 in the initial plasma and steadily increases within the shock front, having an average value of about 1 over the shock front.

Under these conditions ion acoustic waves, most frequently enlisted to explain observed plasma turbulence, should be stable (ion Landau damping is comparatively strong for $T_e \sim T_i$, and $v_d > v_e$ is necessary for instability¹¹). As pointed out by Lashmore and Davies,¹² however, and observed in a computer simulation experiment by Forslund, Morse, and Nielson,¹³ electron-cyclotron waves (Bernstein waves) propagating perpendicular to the magnetic field can become unstable for $T_e \sim T_i$ and $v_d \ll v_e$. The reason for this is that the Doppler-shifted Bernstein wave "sees" a positive slope of the ion distribution function and therefore undergoes inverse Landau damping. Forslund, Morse, and Nielson¹³ have shown that because the instability is resonant with the ions, the maximum growth rate for each harmonic occurs near the crossing of the elec-

tron-wave dispersion curves and the line $\omega/k = v_i$, where v_i is the ion thermal velocity (and not at the ion acoustic phase velocity, as is the case for the ion acoustic instability in the case $T_e/T_i \gg 1$).

Using this result, Gary and Biskamp¹⁴ derived the following expression for the maximum growth rate of this $\vec{E} \times \vec{B}$ electron drift instability

$$\frac{\gamma_{\max}}{\omega_{ce}} \approx 0.368 \frac{T_e v_d - v_i}{T_i v_e} \times \left[\left(1 + k^2 D^2 - 0.075 \frac{T_e}{T_i} \right)^2 + 0.425 \left(\frac{T_e}{T_i} \right)^2 \right]^{-1/2}$$

Inserting our values for conditions at the front of the shock, we get from the above (with $\omega_{ce} = 1.2 \times 10^{10} \text{ sec}^{-1}$)

$$\gamma_{\max} = 1.7 \times 10^8 \text{ sec}^{-1} \text{ for } k=0,$$

and

$$\gamma_{\max} = 0.6 \times 10^8 \text{ sec}^{-1} \text{ for } kD=0.8,$$

corresponding to the wave vector for which the level of turbulence has been measured.

On the other hand, the measured level of fluctuations (250 times the thermal value) implies that

$$e^{\gamma t} = 250$$

or

$$\gamma = 0.9 \times 10^8 \text{ sec}^{-1},$$

in order that the waves grow to the observed level during a time interval of $t = 30 \times 10^{-9} \text{ sec}$ (cf. Fig. 1). Thus the growth rate of the electron drift instability discussed above seems to be sufficient to account for the observed enhanced fluctuations.¹⁵

The phase velocity of the unstable mode observed in the experiment ($\omega \sim 0.5 \times \omega_{pi}$, $kD = 0.8$) agrees well with the result $\omega/k = v_i$ obtained by Forslund, Morse, and Nielson¹³ for unstable electron-cyclotron waves, but would also be a reasonable fit to the dispersion curve for ion acoustic waves. As pointed out by Gary and Biskamp,¹⁴ a possible way of differentiating between these two instabilities is the measure the cone of propagation of the enhanced fluctuations in the $\vec{v}_d - \vec{B}_1$ plane. In the case of an $\vec{E} \times \vec{B}$ electron drift instability, enhanced fluctuations should be concentrated within a few degrees of the drift velocity (as long as nonlinear effects are unimportant), whereas for an ion acoustic instability they should be observed through a broad cone up to about 60° from \vec{v}_d . A light-scat-

tering experiment to test this dependence is in progress.

In summary, the measurements discussed above demonstrate the presence of current-driven turbulence in perpendicular high- β shock waves in which strong, collisionless electron heating has previously been observed. The most interesting result is that the turbulence develops in a plasma with $T_e/T_i \sim 1$ and $v_d/v_e \ll 1$, where ion acoustic waves should be stable. There are good reasons for identifying the instability leading to the observed turbulence with the electron-cyclotron drift instability recently found in a computer simulation experiment¹³ under similar conditions. These results not only have a bearing on collisionless shock waves, but they also suggest that electric currents flowing perpendicular to magnetic field lines in a plasma may, in general, excite an instability, even in the case $T_e \sim T_i$ and $v_d \ll v_e$.

¹J. W. M. Paul, C. C. Daughney, and L. S. Holmes, *Nature* **216**, 363 (1967).

²M. Keilbacker, M. Kornherr, and K.-H. Steuer, *Z. Phys.* **223**, 385 (1969).

³R. Chodura, M. Keilhacker, M. Kornherr, H. Nieder-

meyer, and K.-H. Steuer, in *Proceedings of the Fourth European Conference on Controlled Fusion and Plasma Physics, Rome, Italy, August 1970* (Comitato Nazionale per l'Energia Nucleare, Ufficio Edizioni Scientifiche, Rome, Italy).

⁴K.-H. Steuer and M. Keilhacker, *Bull. Amer. Phys. Soc.* **15**, 1410 (1970).

⁵R. Chodura, M. Keilhacker, M. Kornherr, and H. Niedermeyer, in *Plasma Physics and Controlled Nuclear Fusion Research* (International Atomic Energy Agency, Vienna, Austria, 1969), Vol. I, p. 81.

⁶The initial temperature T_{i1} , which has previously been determined spectroscopically (Ref. 2), has now been measured by collective scattering of laser light.

⁷C. C. Daughney, L. S. Holmes, and J. W. M. Paul, *Phys. Rev. Lett.* **25**, 497 (1970).

⁸S. M. Hamberger and J. Jancarik, *Phys. Rev. Lett.* **25**, 999 (1970).

⁹M. Keilhacker and K.-H. Steuer, to be published.

¹⁰B. B. Kadomtsev, *Plasma Turbulence* (Academic, London, 1965).

¹¹T. E. Stringer, *J. Nucl. Energy, Part C* **6**, 267 (1964).

¹²C. N. Lashmore-Davies, *J. Phys. A: Proc. Phys. Soc.*, London **3**, L40 (1970).

¹³D. W. Forslund, R. L. Morse, and C. W. Nielson, *Phys. Rev. Lett.* **25**, 1266 (1970).

¹⁴S. P. Gary and D. Biskamp, to be published.

¹⁵The authors acknowledge helpful discussions with S. P. Gary on this point.

Effective Charges and Ionicity

P. Lawaetz

Bell Telephone Laboratories, Murray Hill, New Jersey 07974

(Received 24 December 1970)

A simple, empirical connection between electronic and lattice ionicity is reported for 45 $A^N B^{8-N}$ compounds. The Szigeti charge per effective ionic valence is found to be equal to the ratio of Phillips' electronegativity difference C and the plasma energy of the free-valence-electron gas. Deviations are most prominent for low-ionicity compounds containing first-row elements.

The spectroscopic scale of ionicity proposed by Phillips and Van Vechten for the $A^N B^{8-N}$ compounds¹ has successfully correlated a number of important properties of these crystals. This concept of ionicity is based on the electronic low-frequency dielectric constant ϵ_∞ and refers as such to a crystal in equilibrium. In this case, ionicity can be expressed in terms of an ionic contribution C to the average electronic band gap E_g or through the fractional ionicity $f_i = C^2/E_g^2$.

Another manifestation of ionicity is associated with the frequency splitting of the long-wavelength optical vibrations of the lattice and is thus a

property of the strained lattice. Here, ionicity has been described by the relative splitting $(\omega_l^2 - \omega_t^2)/\omega_l^2$,² the normalized splitting S ,³ or various effective charges, notably the Szigeti charge e_s^* .⁴ ω_l and ω_t denote the longitudinal and transverse optical zone-center frequencies, respectively, and

$$S = \frac{(\epsilon_\infty + 2)^2}{9\epsilon_\infty} \left(\frac{e_s^*}{e} \right)^2 = \frac{\Omega\mu}{4\pi e^2} (\omega_l^2 - \omega_t^2), \quad (1)$$

where Ω is the volume of the unit cell, μ is the reduced ionic mass, and e is the elementary charge. The definition of e_s^* involves local-field